Enhancement of Src family kinase activity is essential for p38 MAP kinase-mediated dedifferentiation signal of parotid acinar cells

（p38 MAP キナーゼを介した耳下腺腺房細胞の脱分化シグナルへの Src ファミリーキナーゼの活性上昇の関与）

日本大学松戸歯学部生理学

研究講座員　森山聖子

（指導教授：吉垣純子）

Abstract

Decrease in saliva causes serious problems in clinical dentistry. There have been previous reports on tissue injuries of parotid glands inducing a dedifferentiation signal that causes the loss of function of acinar cells. Since both inhibitors for Src family kinase (SFK) and p38 MAP kinase (p38 MAPK) suppressed the dedifferentiation, SFK-p38 MAPK pathway was considered essential for the signaling. Even though Src and Yes were expressed in the parotid glands, the increase in phosphorylation level was not detected for conserved tyrosine residue in the kinase domain of Src or Yes that promotes kinase activity, following tissue injuries. In this study, the kinase activities were assayed by using the specific substrate for SFK to examine whether the enhancement of kinase activity of SFK was eventuated by tissue injuries. As a result, the activity of the total SFK was elevated after the cellular damage and was sustained for 2 h. To determine the activated SFK member, the SFK activity was examined by immunoprecipitation method with specific antibodies against each SFK member. Elevation of kinase activities of both Src and Yes was detected after cell damages. The elevation ratio of Src activity was higher than Yes, suggesting that the contribution of Src in the dedifferentiation signaling is higher. Diphenyleneiodonium, an NADPH oxidase inhibitor, suppressed the activation of SFK and p38 MAPK, and the expression of claudin-4, a dedifferentiation marker. These results suggest that the activation of SFK is induced by oxidative stresses and is essential for p38 MAPK-mediated dedifferentiation signaling.

Introduction

Saliva plays a significant role in maintaining oral functions such as mastication, articulation and maintenance of oral health. Hence, hyposecretion of saliva and consequent dry mouth cause severe dental caries, periodontitis, and oral mucosa infections. Such salivary dysfunctions are considered to be a serious problem in clinical dentistry (1, 2). The radiotherapy for the treatment of head and neck cancers and autoimmune diseases such as Sjögren syndrome result in the atrophy of acinar cells. Tissue injuries caused by irradiation and inflammation may lead to apoptosis or dysfunction of acinar cells, but the mechanism is unclear. To elucidate the mechanism related to the loss of function of salivary glands, intercellular signals that induce atrophy or dedifferentiation of salivary acinar cells have been studied by using the primary culture of parotid acinar cells.

p38 MAP kinase (MAPK) is known to respond to various tissue damages caused by UV irradiation and oxidative stress. The process of cell isolation from glands using collagenase and hyaluronidase were found to induce the stress signal mediated by p38 MAPK in parotid acinar cells (3). p38 MAPK was phosphorylated, and thus was activated during the process of cell isolation, which was inhibited by Src family kinase (SFK) inhibitors (3). The probable reason is that the enzyme treatment caused tissue injury in parotid glands and triggered the stress signal in acinar cells. The signal of SFK-p38 MAPK has been known to induce the dedifferentiation of parotid acinar cells into duct-like cells (4). Acinar cell markers such as amylase and aquaporin-5 showed a decrease in levels and duct cell markers such as claudin-4 increased during the culture, which were suppressed by inhibitors of SFK and p38 MAPK (3-5). Besides the SFK-p38 MAPK pathway, the signaling pathway via Erk and PKC

were also found to induce dedifferentiation of parotid acinar cells (6). It may be useful to find pathways that induce dysfunction of salivary glands for the development of remedy for xerostomia.

SFK is a family of non-receptor tyrosine kinases including Src, Yes and others. SFK members have a similar domain structure as follows: 1) an N-terminal variable region containing a myristoylation site, 2) a Src homology 3 (SH3) domain, 3) a Src homology 2 (SH2) domain, and 4) a kinase catalytic domain. They also share two conserved tyrosine phosphorylation sites, Tyr^{418} in the kinase domain and Tyr^{529} in the C-terminal tail. Phosphorylated Tyr^{529} residue binds intramolecularly to the SH2 domain, and thus exerts an inhibitory effect on kinase activity (7). Dephosphorylation of Tyr^{529} leads to the dissociation of the C-terminal tail and SH2 domain, resulting in the transition from inactive to active conformation. In contrast, the autophosphorylation of Tyr^{418} in the kinase domain promotes kinase activity (8).

In the previous study, the change in amounts of phosphorylated SFK in the primary culture of parotid acinar cells was examined by using antibodies that specifically recognized phosphorylated SFK at Tyr^{418} and at Tyr^{529}, respectively (8). Although phosphorylated forms of SFK were detected both before and after cell isolation, the alteration in levels of phosphorylation was not observed (3). Hence, it was not determined whether the enhancement of SFK activity was essential for the dedifferentiation signal. In this study, it was examined whether the elevation of SFK activity is required or the basal kinase activity present in parotid glands before tissue injuries is sufficient to induce the signal. In addition, it has been reported that reactive oxygen species (ROS) triggered Erk-PKC signaling pathway that induces acinar dedifferentiation (6). Here, the role of ROS in SFK-p38 MAPK signaling pathway was also

investigated.

Materials and Methods

Preparation and culture of isolated acinar cells

Parotid glands were taken from male Sprague-Dawley rats (150 - 200 g each) anesthetized with sodium pentobarbital. The experiment conformed to the institutional guidelines for the use of experimental animals and was approved by the Experimental Animal Ethical Committee of Nihon University School of Dentistry at Matsudo. Acinar cells were isolated by digestion with collagenase A and hyaluronidase in isolating buffer (Hanks' balanced salt solution adjusted to pH 7.4 with 20 mM HEPES/NaCl buffer) as described previously (9). Since the process of cell isolation takes 1 h, we describe the time point to prepare homogenates of parotid glands before cell isolation as -1 h and that to harvest the cells just after isolation as 0 h in Figs. 2 and 3. The cells were over 90% viable, as was determined by Trypan blue exclusion. The cells were diluted to 0.3 mg/ml with Waymouth's medium containing 10% rat serum, insulin-transferrin-selenium-ethanolamine solution (ITX-S), 1 μM hydrocortisone, 100 U/ml penicillin, 0.1 mg/ml streptomycin and 10 nM cystatin. The medium was changed one day after the cell isolation.

Immunoblot analysis

For immunoblotting analysis, mouse monoclonal anti-Src and anti-Yes antibodies were purchased from Biosource (Camarillo, CA, USA) and BD Biosciences (San Jose, CA, USA), respectively. Goat polyclonal anti-Frk antibody was purchased from Santa Cruz (Santa Cruz,

CA, USA). Mouse monoclonal anti-p38 MAPK antibody and rabbit polyclonal anti-phosphorylated p38 MAPK (T180/Y182) antibody were purchased from BD Biosciences and R & D Systems (Minneapolis, MN, USA), respectively. The cells were washed with phosphate-buffered saline and harvested with Homogenize buffer (150 mM NaCl, 20 mM NaF, 10 mM $MgCl_2$, 1 mM EGTA, 0.1% Triton X-100, 1 × Complete proteinase inhibitor cocktail, and 20 mM HEPES/NaOH, pH 7.4). The same amounts of proteins were applied to each lane of SDS-PAGE: 20 μg for Src, Yes, and Frk, and 8 μg for p38 MAPK and phosphorylated p38 MAPK. The membranes were blocked at room temperature for 50 min in blocking agent (GE Healthcare, Buckinghamshire, UK) and blotted with antibodies. Immunoreactivity was determined by using an ECL Plex and ECF Western blotting kit (GE Healthcare) and the images were acquired using with Typhoon Trio (GE Healthcare).

Immunoprecipitation

Cell lysates were solubilized with lysis buffer (150 mM NaCl, 20 mM NaF, 10 mM $MgCl_2$, 1 mM EGTA, 1% Triton X-100, 0.25% sodium deoxycholate, 1 × Complete proteinase inhibitor cocktail, and 20 mM HEPES/NaOH, pH 7.4). For immunoprecipitation of SFK, rabbit polyclonal anti-Src (Abcam, Cambridge, UK), anti-Yes (Santa Cruz) and anti-Frk (Proteintech, Chicago, IL, USA) antibodies were used. Each antibody (2 μg) was added to protein A-Sepharose 4FF and was incubated at 4 °C for 60 min. After washing with lysis buffer, the solubilized samples (30 μg) were added to antibodies-conjugated protein A-Sepharose 4FF and were incubated at 4 °C for 2 h. Following this, precipitates were collected by centrifugation and washed with lysis buffer.

Assay of SFK activity

SFK activity was determined with CycLex® c-Src Kinase Assay/Inhibitor Screening Kit (Cyclex, Nagano, Japan) according to the manufacturer's instructions. For the total SFK activity assay, lysate of 0.5 μg each was used. To assay for the activity of each SFK member, suspension of immunoprecipitated Sepharose beads was added to the well. The phosphorylated substrates were quantified by measuring the absorbance at 450 nm with microplate reader MTP-450 (Hitachi Hi-Tech Science, Tokyo, Japan).

RNA preparation and real time RT-PCR analysis of mRNA expression.

Total RNA was isolated from parotid acinar cells immediately after their isolation, or after 2 h in culture, using the TRIzol reagent (Invitrogen). After treatment with DNase I, RNA was purified with RNeasy Mini kits (Qiagen). RNA was quantified by measuring the absorbance at 260 nm. The expression levels were determined with the QuantiTect® SYBR® RT-PCR kit (Qiagen) using the DNA Engine Opticon™ System (MJ Research, Waltham, MA). Primer pairs for amplification of rat *Gapdh* and *Cldn4* of the rat were designed according to a previous study (5). The PCR products were evaluated by melting curve analysis according to the manufacturer's instructions and by examining the size of the PCR products separated on 2.0% agarose gel. Relative RNA equivalents for each sample were obtained by normalizing to *Gapdh* levels. Each sample was run in duplicates to determine sample reproducibility, and the average relative RNA equivalents per sample pair were used for further analysis.

Results

Expression pattern of SFK in parotid acinar cells

Firstly, the member of SFK that was expressed in parotid acinar cells was confirmed. Immediately after the isolation of acinar cells, specific antibodies against Src and Yes detected bands at the apparent molecular weights of about 60 kDa (Fig. 1). An elevated proportion of the expressed protein levels was observed in the cultured cells as reported previously (3). Frk was scarcely observed just after the cell isolation, and a band at the molecular weight of about 55 kDa became detectable after one-day culture. The molecular weights of the detected bands were consistent with the expected ones. The antibodies were also used against other members of the SFK such as Fyn, Lyn, Lck, Hck or Fgr, which were not detected (data not shown).

Alteration of SFK activity during the cell isolation and culture

Since the inhibition of SFK activity by inhibitors, PP1 and SU6656, suppressed the dedifferentiation of parotid acinar cells (3), the kinase activity holds importance in inducing the dedifferentiation signal. However, the change in phosphorylated levels of Src and Yes could not be detected between the pre- and post-treatment of collagenase and hyaluronidase by immunoblot analysis (3). Subsequently, the kinase activity to phosphorylate the specific substrate for SFK was directly measured. The SFK activity in homogenates of parotid glands (-1 h) and acinar cell lysate just after treatment with enzymes (0 h) were found to be 0.81 ± 0.10 and 2.30 ± 0.33 units/μg proteins, respectively (Fig. 2). The result showed that the treatment of enzymes for cell isolation led to cell damages and induced the enhancement of SFK activity. The kinase activity was shown to decline subsequently and reached almost the same level as before the cell isolation (Fig. 2).

It has been previously found that diphenyleneiodonium (DPI), an NADPH oxidase inhibitor, suppressed the activation of Erk induced by the process of cell isolation (6). Then, the involvement of oxidative stress in SFK activity was examined. In the presence of DPI, the activation of SFK was suppressed (Fig. 2). The activity at 6 h became lower prior to the cell isolation. This result suggested that oxidative stress induced by tissue injury during isolation caused SFK activation.

Activation of the members of SFK during the process of cell isolation

To determine the member of SFK involved in the dedifferentiation signal, each member was immunoprecipitated with a specific antibody, and the precipitates were used for kinase assay (Fig. 3). As a result, kinase activities of both Src and Yes were elevated upon the process of cell isolation. The activity of Src was declined and reached to the control level at 6 h after the isolation. The ratio of Yes activation from before (-1 h) to after (0 h) cell isolation was lower than that of Src and its activity scaled up once more at 24 h. The elevation in the activity at 24 h may be due to the increase of protein level of Yes after one day of culture (Fig. 1). In contrast, the activity of Frk was not changed during the process of cell isolation. Its activity was gradually increased during the culture. The change of the Frk activity was consistent with the expression level of the Frk protein (Fig. 1).

Effect of DPI on SFK activities

The effect of DPI on each member of SFK was examined. The lysates from the cells just after isolation (0 h) and those cultured for 2 h and 24 h were harvested (Fig. 4). After immunoprecipitation with specific antibodies against Src, Yes and Frk, the kinase activity was

determined. DPI was found to inhibit partially the activation of Src and Yes just after the isolation (0 h). At 2 h, the activities of Src and Yes in the presence of DPI were declined to the control level before cell isolation. Since Frk was not activated after isolation, there was no effect of DPI on Frk activity at 0 h. After 24 h-culture in the presence of DPI, the kinase activity of Frk was suppressed below the control level before isolation.

Effect of DPI on the p38 MAPK activity and expression of claudin-4

It has been previously reported that p38 MAPK was activated with the process of cell isolation, which was suppressed by SFK inhibitors (3). Those results suggested that p38 MAPK was present downstream of SFK signaling. To confirm this, the effect of DPI on activation of p38 MAPK was examined. The phosphorylated form of p38 MAPK was increased during cell isolation and was sustained up to 2 h while the total amount of p38 MAPK was not changed as previously reported (3). In the presence of DPI, the phosphorylated form of p38 MAPK was decreased compared to the conditions in the absence of DPI (Fig. 5A). Therefore, the activation of SFK is necessary for the dedifferentiation signal mediated by p38 MAPK in parotid acinar cells.

As previously reported, the expression levels of acinar cells markers were declined after tissue injuries and duct cell markers such as claudin-4 began to be expressed concomitantly (5). It was found that the SFK inhibitors such as PP1 suppressed the change in gene expression (3). To confirm whether decrease in the oxidative stress suppressed the dedifferentiation signal, the effect of DPI on the expression of claudin-4 mRNA was investigated. The expression level of claudin-4 in isolated acinar cells (0 h) was low and increased to more than 10-fold after 2 h of culture in the absence of PP1 and DPI (control).

Addition of PP1 or DPI significantly reduced the expression of claudin-4 (Fig. 5B), suggesting that DPI suppressed the dedifferentiation of parotid acinar cells as well as SFK inhibitors.

Discussion

The present study confirmed the enhancement of SFK activity in parotid acinar cells upon the process of cell isolation. In the previous study, the above-mentioned phenomenon was examined by immunoblot analysis with anti-phospho-Tyr^{418} and anti-phospho-Tyr^{529} Src antibodies that recognized phosphorylated tyrosine residues in the kinase domain and in the C-terminal domain, respectively. The phosphorylation of Tyr^{418} indicates the activation of SFK (8) and dephosphorylation of Tyr^{529} causes a conformational change, which is necessary for their activation (10). The phosphorylation of C-terminal tyrosine residue was mainly driven by Csk (11). As the difference between the amounts of phosphorylated Src and Yes before and after cell isolation remained undetected by immunoblot analysis, it was difficult to determine whether the activities of SFK were enhanced. In this study, the kinase activities of Src and Yes were elevated just after isolation and were sustained for 2 h (Fig. 3). This discrepancy between the results of immunoblot analysis and kinase assay may be due to the SFK activities that have been enhanced to some extent before the cell damage (Fig. 2). The result is consistent with a previous report stating that phosphorylation of Tyr^{418} residue of Src and Yes was observed even in homogenates of the control parotid glands (3). This may have made the detection of the change in amounts of phosphorylated forms difficult. Another

possibility is that the regulatory mechanism of SFK activity in this signaling pathway is independent of the phosphorylation of tyrosine residues. ROS directly oxidize cysteine residues of SFK, which results in the formation of a disulfide bond between SH2 and kinase domains of SFK. The conformational change induces their activation (12). In fibroblast cell lines, ROS activates both Csk and Src, and therefore tyrosine kinase activity is enhanced without decrease of the phosphorylation level of Tyr^{529} of Src (13).

The suppression of the activation of SFK by DPI suggests that ROS is upstream of SFK signaling (Figs. 2 and 4). In many types of cells, ROS is involved in cellular signaling. Angiotensin II induces epithelial-mesenchymal transition in renal epithelial cells by activation of Src, which needs a generation of ROS (14). Low-power laser irradiation also activates Src through ROS signaling pathway (15). On the other hand, there are inconsistent reports that Src activates NADPH oxidase (16), and its kinase activity is essential for the generation of ROS (17, 18), suggesting that the involvement of various signaling pathways in ROS and SFK. The ROS signaling may also have a positive feedback cycle of response to stress and tissue damages. The proposed mechanism of SFK activation by ROS states that ROS oxidizes and inactivates protein tyrosine phosphatases that suppress SFK activity (19). ROS can also oxidize cysteine residues of Src, which directly leads to SFK activation. The activation of Src by oxidation is considered to be maintained longer (for at least 3 h) than the activation by phosphorylation (20). In this study, the activity of SFK was sustained for 2 h and the result was consistent with the previous reports.

Since Src inhibitors suppressed the activation of p38 MAPK, it was predicted that SFK is upstream of p38 MAPK signaling (3). In this study, the effects of DPI on activation of SFK and p38 MAPK were similar. After 2 h-culture in the presence of DPI, SFK activity was

declined to the control level before cell isolation (Figs. 2 and 4), and coincidently, the phosphorylation level of p38 MAPK was significantly decreased (Fig. 5A). These results suggested that ROS activated p38 MAPK via activation of SFK. The control level of SFK activity was insufficient to maintain activation of p38 MAPK.

The increase in activity of Src was higher than that of Yes (Fig. 3). It is likely that the contribution of Src in the dedifferentiation signal was larger. The enhancement of kinase activities of both Src and Yes were declined at 6 h. In the presence of DPI, the activity of Src and Yes decreased to almost the same level as before isolation (Fig. 4). It has been reported that incubation with SFK inhibitors for only first 24 h was sufficient to suppress the dedifferentiation of parotid acinar cells, suggesting that signaling mediated by SFK was finished within 24 h (3). The result in this study explains the effect of inhibitors in the previous study. This study suggests the possibility that the dysfunction of salivary acinar cells could be rescued by inhibition of this signaling pathway in the early stage.

Acknowledgements

This work was supported in part by the Nihon University Multidisciplinary Research Grant for 2011, a grant for Supporting Project for Strategic Research by MEXT, 2008-2012 (S0801032) and a grant from Research Institute of Oral Science, Nihon University School of Dentistry at Matsudo (B-03).

References

1. Sreebny L: Xerostomia: Diagnosis, management and clinical complications. In: Saliva and oral health (2nd ed.), Edgar W and O'Mullane D ed. British Dental Association, London, 1996, p. 45-50.

2. Baum BJ: Prospects for re-engineering salivary glands. Adv Dent Res, 14: 84-88, 2000.

3. Fujita-Yoshigaki J, Matsuki-Fukushima M, and Sugiya H: Inhibition of Src and p38 MAP kinases suppresses the change of claudin expression induced on dedifferentiation of primary cultured parotid acinar cells. Am J Physiol Cell Physiol, 294: C774-C785, 2008.

4. Fujita-Yoshigaki J, Qi B, Narita T, and Sugiya H: Parotid acinar cells transiently change to duct-like cells during epithelial-mesenchymal transition. J Med Invest, 56 Suppl: 258-259, 2009.

5. Qi B, Fujita-Yoshigaki J, Michikawa H, Satoh K, Katsumata O, and Sugiya H: Differences in claudin synthesis in primary cultures of acinar cells from rat salivary gland are correlated with the specific three-dimensional organization of the cells. Cell Tissue Res, 329: 59-70, 2007.

6. Inoue D, Yokoyama M, and Katsumata-Kato O: Tissue injury-induced reactive oxygen species cause dysfunction of parotid acinar cells via Erk-novel PKC activation. Int J Oral Med Sci, 13: 6-11, 2014.

7. Okada M, Howell BW, Broome MA, and Cooper JA: Deletion of the SH3 domain of Src interferes with regulation by the phosphorylated carboxyl-terminal tyrosine. J Biol Chem, 268: 18070-18075, 1993.

8. Smart JE, Oppermann H, Czernilofsky AP, Purchio AF, Erikson RL, and Bishop JM:

Characterization of sites for tyrosine phosphorylation in the transforming protein of Rous sarcoma virus (pp60v-src) and its normal cellular homologue (pp60c-src). Proc Natl Acad Sci USA, 78: 6013-6017, 1981.

9. Fujita-Yoshigaki J, Tagashira A, Yoshigaki T, Furuyama S, and Sugiya H: A primary culture of parotid acinar cells retaining capacity for agonists-induced amylase secretion and generation of new secretory granules. Cell Tissue Res, 320: 455-464, 2005.

10. Nada S, Okada M, MacAuley A, Cooper JA, and Nakagawa H: Cloning of a complementary DNA for a protein-tyrosine kinase that specifically phosphorylates a negative regulatory site of p60c-src. Nature, 351: 69-72, 1991.

11. Okada M, Nada S, Yamanashi Y, Yamamoto T, and Nakagawa H: CSK: a protein-tyrosine kinase involved in regulation of src family kinases. J Biol Chem, 266: 24249-24252, 1991.

12. Giannoni E, Buricchi F, Raugei G, Ramponi G, and Chiarugi P: Intracellular reactive oxygen species activate Src tyrosine kinase during cell adhesion and anchorage-dependent cell growth. Mol Cell Biol, 25: 6391-6403, 2005.

13. Cao H, Sanguinetti AR, and Mastick CC: Oxidative stress activates both Src-kinases and their negative regulator Csk and induces phosphorylation of two targeting proteins for Csk: caveolin-1 and paxillin. Exp Cell Res, 294: 159-171, 2004.

14. Chen J, Chen JK, and Harris RC: Angiotensin II induces epithelial-to-mesenchymal transition in renal epithelial cells through reactive oxygen species/Src/caveolin-mediated activation of an epidermal growth factor receptor-extracellular signal-regulated kinase signaling pathway. Mol Cell Biol, 32: 981-991, 2012.

15. Zhang J, Xing D, and Gao X: Low-power laser irradiation activates Src tyrosine kinase through reactive oxygen species-mediated signaling pathway. J Cell Physiol, 217: 518-528,

2008.

16. Chowdhury AK, Watkins T, Parinandi NL, Saatian B, Kleinberg ME, Usatyuk PV, and Natarajan V: Src-mediated tyrosine phosphorylation of p47phox in hyperoxia-induced activation of NADPH oxidase and generation of reactive oxygen species in lung endothelial cells. J Biol Chem, 280: 20700-20711, 2005.

17. Wagner B and Gorin Y: Src tyrosine kinase mediates platelet-derived growth factor BB-induced and redox-dependent migration in metanephric mesenchymal cells. Am J Physiol Renal Physiol, 306: F85-97, 2013.

18. Lee IT, Wang SW, Lee CW, Chang CC, Lin CC, Luo SF, and Yang CM: Lipoteichoic acid induces HO-1 expression via the TLR2/MyD88/c-Src/NADPH oxidase pathway and Nrf2 in human tracheal smooth muscle cells. J Immunol, 181: 5098-5110, 2008.

19. Gross S, Knebel A, Tenev T, Neininger A, Gaestel M, Herrlich P, and Bohmer FD: Inactivation of protein-tyrosine phosphatases as mechanism of UV-induced signal transduction. J Biol Chem, 274: 26378-26386, 1999.

20. Xi G, Shen XC, Wai C, and Clemmons DR: Recruitment of Nox4 to a plasma membrane scaffold is required for localized reactive oxygen species generation and sustained Src activation in response to insulin-like growth factor-I. J Biol Chem, 288: 15641-15653, 2013.

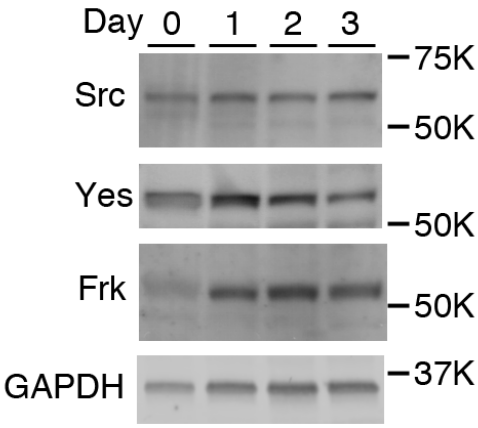

Figure 1 Expression of the SFK in parotid acinar cells

Cells were harvested just after (0) and at 1-3 days after isolation. Cell lysates (20 μg each) were loaded to 7.5% SDS-PAGE, transferred and visualized using a polyclonal anti-Src, anti-Yes or anti-Frk antibodies. As a reference protein, the expression level of GAPDH was also examined.

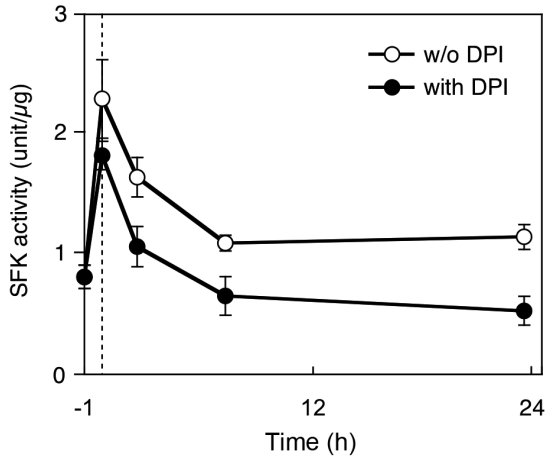

Figure 2 Enhancement of SFK activity in primary culture of parotid acinar cells

Homogenates of parotid glands (-1 h) were prepared. The cells were harvested after (0 h) isolation, and after culture for 2, 6 and 24 h in the presence or absence of 10 μM DPI. All values are shown as means ± SE (n = 4). In the presence of DPI, the SFK activity is significantly lower than in its absence (*$P < 0.05$, two-way ANOVA).

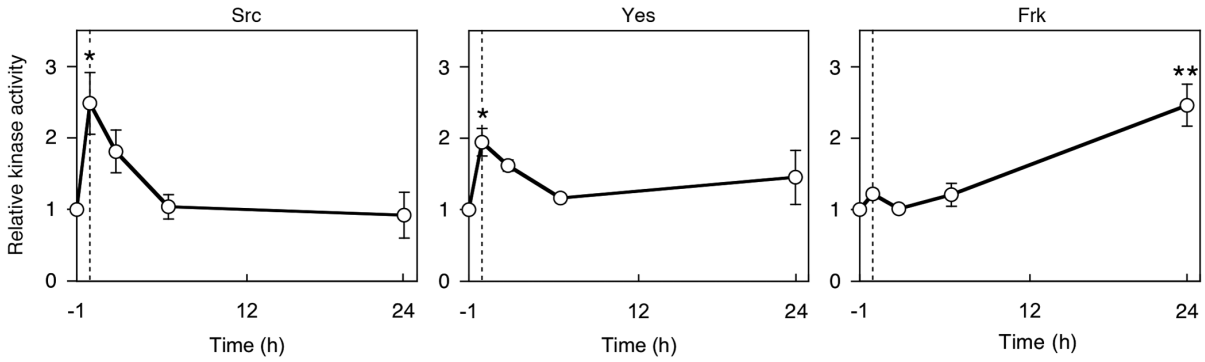

Figure 3 Change in kinase activity of each SFK member

After immunoprecipitation with each specific antibody from the lysates harvested at each time point, suspensions of precipitates were used for the assay (n = 3). The relative values to the activity before cell isolation (-1 h) were shown (**$P < 0.01$, *$P < 0.05$ vs before isolation, one-way ANOVA with Dunnett's multiple comparison test; n = 3).

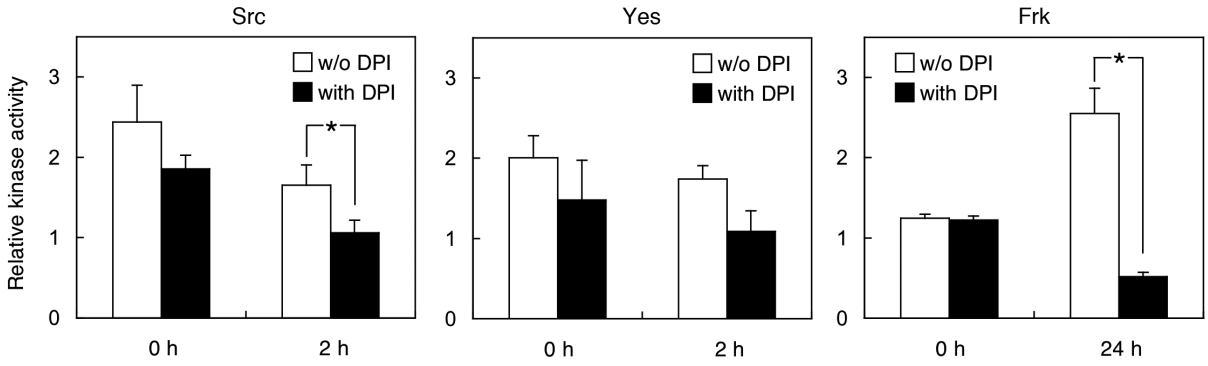

Figure 4 Effect of DPI on the kinase activity of SFK

Immunoprecipitates from the lysates of the cells untreated or treated with DPI were used for the assay. The relative values to the activity before cell isolation were shown (*$P < 0.05$ vs without DPI, paired *t*-test; n = 3).

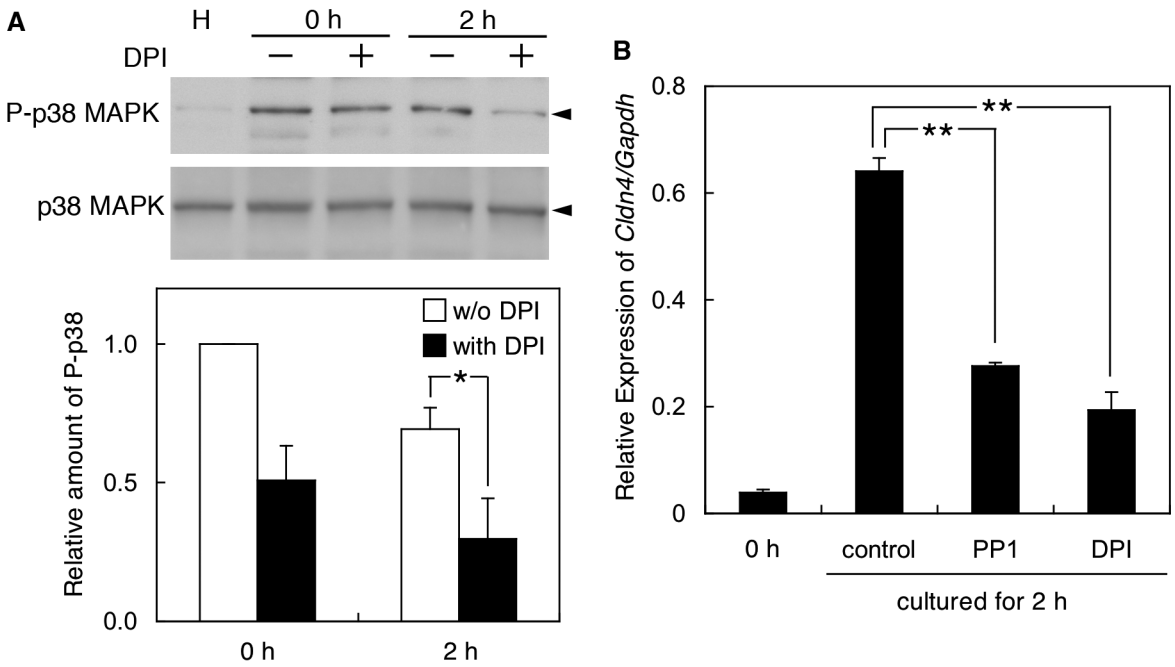

Figure 5 Effect of DPI on the dedifferentiation signal via p38 MAPK.

A. Acinar cells isolated without (-) or with 10 μM DPI (+) were harvested just after isolation (0 h) and after culture for 2 h (2 h). A homogenate of parotid glands (H), and cell lysates (8 μg each) were used for immunoblot analysis by antibodies against phosphorylated form (P-p38 MAPK), and total p38 MAPK. Quantitative analyses of immunoblots showed that incubation with DPI during the cell isolation decreased the phosphorylated form of p38 MAPK. (*P < 0.05 vs without DPI, paired t-test; n = 3). B. The expression level of claudin-4 (*Cldn4*) was increased after the culture for 2 h (control) compared to just after cell isolation (0 h). The increase was suppressed in the presence of 10 μM PP1 or 10 μM DPI (*P < 0.01 vs control, one-way ANOVA with Dunnett's multiple comparison test; n = 3).